





Research Article

Real-Time Predictive Energy-Saving Control for Electric Vehicle Based on Road Slope Prediction

Dongmei Wu ^{1,2,3}, Zhenfeng Lin ^{1,2,3}, Changqing Du ^{1,2,3} and Yang Li ⁴

¹Hubei Key Laboratory of Advanced Technology for Automotive Components, Wuhan University of Technology, Wuhan 430070, China

²Foshan Xianhu Laboratory of the Advanced Energy Science and Technology Guangdong Laboratory, Foshan 528200, China

³Hubei Research Center for New Energy Intelligent Connected Vehicle, Wuhan University of Technology, Wuhan 430070, China

⁴Technical Center of Dongfeng Commercial Vehicle, Wuhan 430056, China

Correspondence should be addressed to Changqing Du; cq_du@whut.edu.cn

Received 21 November 2022; Revised 12 March 2023; Accepted 20 June 2023; Published 14 October 2023

Academic Editor: Gianluca Coccia

Copyright © 2023 Dongmei Wu et al. This is an open access article distributed under the Creative Commons Attribution License, which permits unrestricted use, distribution, and reproduction in any medium, provided the original work is properly cited.

Predictive energy-saving control (PEC) is aimed at reducing energy consumption by designing the vehicle speed while considering future road and traffic information. In particular, the slope of the road ahead is necessary and critical for PEC. This paper proposes a road slope prediction method for production vehicles that uses the nonlinear autoregressive (NAR) neural network model based on road slope sensors. To adaptively balance the energy savings and trip time, this paper proposed a real-time variable weight PEC method for a four-wheel-drive (4WD) intelligent electric vehicle. The weight coefficients are automatically changed according to the characteristics of the road slope, where the vehicle energy-saving rate on the steep downhill road can be maximized. The results of real-time simulation on the dSPACE platform indicated that the road slope predictive model can be run in real time and adapted to changes in road slope and speed. The root mean square error (RMSE) of the predictive results is 0.3063. On a steep downhill road, the energy-saving rate of the proposed PEC method can reach 30.87% at a small expense of time of 3.75%. On uphill and flat roads, energy can be saved by 6.35% at a time cost of 3.0%. Compared with the PEC with constant weight factors, the two control objectives of energy savings and traveling time can be better balanced on various types of roads.

1. Introduction

Currently, electric vehicles and autonomous vehicles are hot topics for the vehicle industry and for researchers [1–3]. Motivated by these trends, advanced driving assistance systems (ADAS) have been rapidly developing in recent decades. These systems feature a series of autonomous control functions for driving assistance and safety enhancement [4, 5]. In the vehicle longitudinal direction, ACC is an essential system to automatically control the vehicle speed according to the traffic environment. In addition, fuel economy is one of the most important aspects of vehicles and has always been a focus in the automotive field. Therefore, ACC systems are being researched not only to improve the ride comfort and safety performance of vehicles but also to reduce energy consumption [6, 7].

Currently, research on energy savings in ACC systems focuses on two strategies. The first strategy, known as efficiency ACC (EACC), consists of reducing the instantaneous acceleration or enhancing the energy efficiency of the driving system. This method can reduce the instantaneous energy consumption, but the energy economy on the entire route or in a section of the journey cannot be controlled [8, 9]. The second strategy consists of programming and controlling the vehicle speed in a horizon based on the knowledge of future road conditions, such as the road slope, speed limit, and traffic signals; this strategy is usually known as predictive energy-saving control (PEC). This approach can save energy when added to the results of the first method. Therefore, PEC has recently attracted much attention.

For PEC, information on future road conditions can be used in vehicle speed programming to help reduce the fuel

consumption and energy needs. For example, vehicle speed usually increases when going downhill, and the driver needs to brake to maintain the speed. If the change in the road slope is known in advance, vehicles can be slowed down before going downhill by easing the acceleration pedal. Then, the velocity will increase to a higher value on the downhill slopes without braking or by light braking. Therefore, the kinetic energy dissipated into heat can be reduced by reducing unnecessary braking, which lowers the aggregate energy consumption [10]. PEC was first introduced in heavy vehicles. The test results in references [11, 12] show that PEC can reduce fuel consumption by more than 3% compared to conventional ACC. For hybrid electric vehicles, PEC can be effectively employed in energy management strategies with obvious energy savings potential [13, 14]. PEC is also critical for alleviating mileage anxiety for electric vehicles (EVs) [15].

The road inclination is an essential piece of information of the future road and is vital for PEC. Usually, two approaches are used to assess the road slope: a digital map that stores road slope information or slope estimation. In many previous studies, the road grade is assumed to be available from a map with stored road information [16, 17]. Combining vehicle positioning via a global positioning system (GPS), reference [18] obtained the slope of the future road by recalling the high-definition map according to the future location of the vehicle. However, the application of high-precision maps in production vehicles is currently limited by their high cost. In addition, high-definition maps are primarily collected for certain areas or routes. For vehicles not equipped with information stored in maps or vehicles driving on roads without maps, slope estimation methods are usually used. The sensor configuration for intelligent vehicles has been developing quickly, such as cameras, radar, lidar, laser/inertial profilometers, and differential GPS systems [19–21]. Some advanced estimation approaches with sensor fusion have also been proposed [22–24], but these sensors are too costly for production vehicles at present. In reference [25], the road grade model is construed stochastically as a Markov chain. However, the transition probabilities depend on the measured data for the road slope in a specific area. Other control systems refer to road slope estimation based on the vehicle dynamics model [26–28]. However, this type of approach can only estimate the current road inclination and not the grade on the forward road.

As discussed above, the currently available methods to obtain the road slope based on map data or slope estimation are not suitable for a wide range of applications in various regions. The acquisition of gradient information on various roads is a considerable challenge for PEC application in production vehicles. Fortunately, with the development of automatic control systems, vehicles are being equipped with more on-board sensors, such as the road slope sensor, which can measure the instantaneous road slope in real time. Currently, data-based models are increasingly being widely used to estimate vehicle states and parameters and predict future information based on historical data with machine learning methods [29–31]. In particular, the nonlinear autoregressive (NAR) neural network presents fast convergence along with

good capability due to its feedback control structure [32, 33]. Motivated by this background, this paper proposes a road grade prediction method based on onboard road slope sensors. The data of the measured road slope are recorded for a period of time as the vehicle travels. Due to the continuity of the elevation of the road, an NAR neural network model is established to obtain the future road slope based on the slope of the backward road. In this way, the road slope can be obtained on various roads, even when terrain data are lacking. This approach provides a practical solution for PEC on vehicles without high-definition maps.

For PEC, MPC is usually used to reduce the energy consumption while minimizing the trip time. However, the two performances are usually in conflict, and the balance between them must be considered through different weights. Therefore, the weight factors of different cost functions are significant to the control performance. In previous research, the weight factors are constant or not introduced in detail [12, 18]. Reference [12] mentioned that more energy may be saved in a hill area than in a flat area. Nevertheless, the weight factors can only be adjusted by drivers in this reference. Reference [34] concluded that much energy can be saved on a steep downhill road. Therefore, the coefficients of the cost objectives are set to larger values on steep downhill roads than in other stages. Compared with PEC with constant weight factors, the general performance in different road conditions can be improved. However, only offline simulations were conducted, and real-time running was not verified in this study.

For the real-time application of PEC on road vehicles, the calculation load must be evaluated. Specifically, the verification of data-based methods in real-time control systems is rare. This paper integrates the NAR slope estimation algorithm into the variable weight PEC algorithm simulated in reference [34]. The complete PEC system is tested on the dSPACE real-time simulation platform. The real-time computing capability of this algorithm is validated, which is an important prerequisite for practical application in real vehicles.

In summary, the road slope of the future road is necessary information for PEC, but this information is difficult to obtain for production vehicles in a manner that is low in cost and widely adaptable. The current methods based on map data or slope estimation are not suitable for mass applications on vehicles in various regions. This paper proposes a road slope prediction method using an on-board road slope sensor that can be installed on production vehicles at a low cost. Based on the recorded slope of the road passed before a period of time, the NAR neural network is adopted to establish the road slope predictive model because of its high accuracy and good capability. Using the predicted road slope, this paper devised a variable weight PEC algorithm to balance the energy consumption and travel time. Because machine learning algorithms are rarely applied in real-time control systems, this paper tested the entire control system in the dSPACE real-time platform. This work provides an important reference for the practical application of PEC systems in vehicles.

The remainder of the paper is organized as follows: the PEC framework and variable weight control algorithm are

presented in Section 2. The road slope prediction based on the NAR neural network is introduced in Section 3. The results of real-time simulation on the dSPACE platform are given in Section 4. The discussions are shown in Section 5, and the conclusions are indicated in Section 6.

2. Variable Weight PEC Method

2.1. PEC Framework. As shown in Figure 1, the PEC system generally consists of four sections: the vehicle sensor system, the vehicle motion decision module, the PEC module, and the actuator module. In the vehicle sensor system, the environmental perception sensors identify the target vehicle and obtain the relative distance and relative speed between the host vehicle and the target vehicle. The vehicle state sensor can obtain the longitudinal speed, lateral speed, and yaw rate of the ego vehicle. The road gradient sensor can obtain real-time gradient information for the road. The vehicle motion decision module determined the reference vehicle speed according to the motion of the preceding vehicle and the host vehicle. Because this module is no different from the traditional ACC, this paper will not introduce it in detail.

Based on the reference vehicle speed determined by the vehicle motion decision module, the PEC module optimizes the desired speed according to the road slope. Based on the historical gradient information obtained by the road slope sensor, the neural network algorithm is used to predict the future gradient. With the road slope information, the vehicle longitudinal dynamics model and the energy consumption prediction model are established. Considering the travel time and energy consumption cost terms, the MPC method is used to perform vehicle speed prediction control. The desired torque of the vehicle is determined and output to the actuators. This paper focuses on the adjustment of the weight coefficient, which will be described in detail in the following section.

In the actuator module, the desired driving or braking torque is generated by the driving motor or the mechanical braking system. Notably, braking energy recovery is not considered in this paper. Therefore, the driving torque is realized by the drive motor, and the braking torque is generated by the hydraulic braking system.

In summary, this paper focuses on the PEC module, including road gradient prediction and MPC speed predictive control, as shown in Figure 1. Other modules are not further described in this paper.

2.2. PEC Problem Formulation. First, the longitudinal dynamics model is established as

$$\begin{bmatrix} \dot{x}_1 \\ \dot{x}_2 \end{bmatrix} = \begin{bmatrix} x_2 \\ \frac{1}{\delta m} \left(u/r - g(f \cos \alpha + \sin \alpha) - \frac{1}{2} C_D A \rho x_2^2 \right) \end{bmatrix}, \quad (1)$$

where the state variable is $\mathbf{x} = [x_1 \ x_2]^T$, x_1 is the vehicle speed, and x_2 is the traveling displacement. δ is the rotational mass conversion factor. m is the vehicle mass. The control input

$u = T_w$ is the required vehicle torque. For 4WD EVs with four distributed driven wheels, $T_w = \sum_{i=1}^4 T_i \cdot g$ is the gravitational acceleration. f is the rolling resistance coefficient. α is the road slope angle. C_D is the air drag coefficient, A is the vehicle windward area, and ρ is the air density.

Based on the control input in Equation (1), the energy prediction model can be expressed in

$$\dot{E}(t) = \begin{cases} \sum_{i=1}^4 (T_i n + P_l(T_i, n)), & T_i \geq 0, \\ 0, & T_i < 0, \end{cases} \quad (2)$$

where n is the wheel revolution speed, $T_i = T_w/4$ is the output moment of each driven motor, and $P_l(T_i, n)$ is the real-time power loss of the electric motor, which can be obtained from motor efficiency data.

Based on Equation (1) and Equation (2), the PEC optimal problem can be formulated as

$$\begin{aligned} \min J &= \int_0^T \left(\lambda_p (\dot{E}(t))^2 + \lambda_v (x_2(t) - v_{\text{ref}}(t))^2 \right) dt, \\ \text{s.t. } \begin{bmatrix} \dot{x}_1 \\ \dot{x}_2 \end{bmatrix} &= \begin{bmatrix} x_2 \\ \frac{1}{\delta m} \left(\frac{u}{r} - g(f \cos \alpha + \sin \alpha) - \frac{1}{2} C_D A \rho x_2^2 \right) \end{bmatrix}, \\ \dot{E}(t) &= \begin{cases} \sum_{i=1}^4 (T_i n + P_l(T_i, n)), & T_i \geq 0, \\ 0, & T_i < 0, \end{cases} \\ T_{\min} &\leq T_i \leq T_{\max}, \end{aligned} \quad (3)$$

where T is the prediction horizon, $v_{\text{ref}}(t)$ is the reference speed, T_{\min} and T_{\max} are the minimum and maximum output torque of each driven motor, and λ_p and λ_v are the coefficients of each cost objective. The first part of the objective function denotes the minimum energy consumption, and the second part of the objective function represents the minimum speed following deviation.

As described in [34], much energy can be saved on a sharply descending road. The coefficients of cost objectives are set to larger values on this type of road than on other stages, as follows:

$$\begin{aligned} \lambda_p &= 0.1, & \text{sharp descending road,} \\ \lambda_p &= 0.5, & \text{sharp ascending road,} \\ \lambda_p &= 0.1, & \text{small uneven road.} \end{aligned} \quad (4)$$

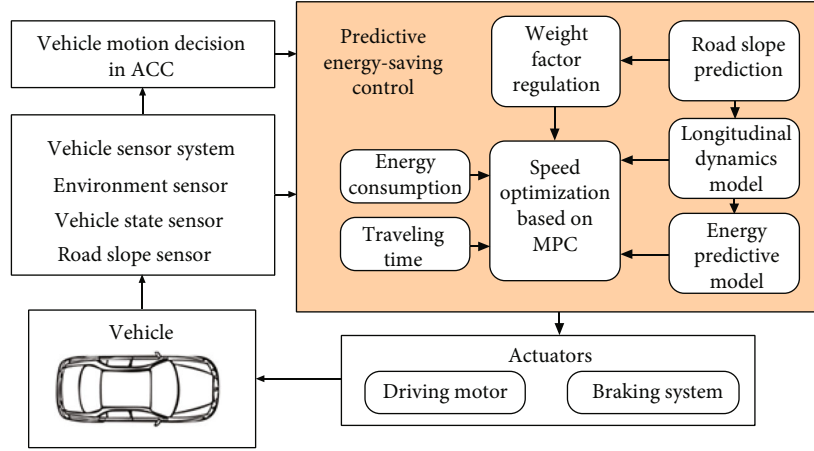


FIGURE 1: The framework of PEC.

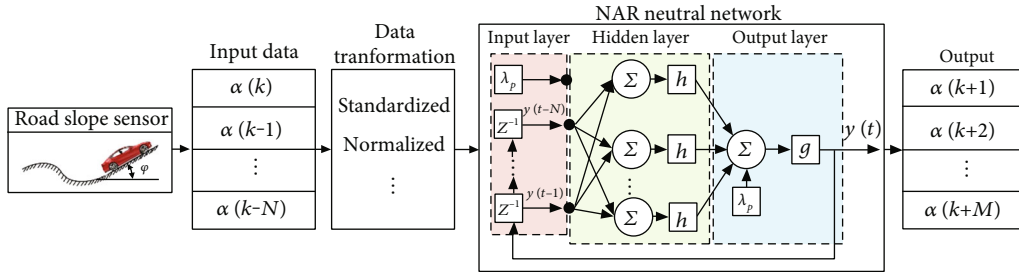


FIGURE 2: Diagram of the road slope predictive model based on the NAR neural network.

For the types of roads in Equation (4), steep downhill roads need to be distinguished from the other two types of roads according to

$$\begin{aligned} &\theta(i-1) \cdot \theta(i) < 0, \\ &\forall \theta(i) > 0 \quad \{k \in Z | (i-200) \leq k < i\}, \end{aligned} \quad (5)$$

where $\theta(i)$ is the road gradient at the present control step i .

The computational load of MPC optimization problems has always been an important issue. To achieve real-time running, a fast-solving method based on the projected gradient algorithm was selected to solve the above optimization problem. It was integrated in the tool named gradient-based MPC (GRAMPC) [35].

3. Road Slope Prediction Based on the NAR Neural Network

3.1. NAR Neural Network Algorithm Design. Because the road slope is fixed based on the location of the road, it should change with the displacement of the vehicle. However, measuring the slope with a constant distance interval is challenging for road slope sensors. Comparably, measuring the data is easy for a fixed time interval. Consequently, we predicted the road gradient based on the road slope-time data series rather than the road slope-displacement data series, despite the inevitable effect of speed. The predictive results for different vehicle speeds are validated in the following. Artificial neural networks have excellent nonlin-

ear fitting ability and have great advantages when solving nonlinear and time-varying problems. At present, many types of neural networks have been applied to analyze and predict time series. Particularly, the NAR network, a type of dynamic neural network, is suitable for the prediction of time series. Previous studies have shown its advantages in terms of small computation times and high prediction accuracy [36]. Therefore, the NAR neural network was used in this study to establish a slope prediction model based on the slope time series.

The NAR neural network is a type of nonlinear regression model used to describe a future variable based on a nonlinear combination of variables used in the previous period. The mathematical expression is given by

$$y(t) = f(y(t-1), y(t-2), y(t-3) \cdots y(t-n)), \quad (6)$$

where $y(t)$ is the output of the neural network and $y(t-1), y(t-2), y(t-3) \cdots y(t-n)$ are the input data of the past n steps.

The NAR neural network uses past data as input. Future prediction information is obtained through the nonlinear calculation of the hidden layer and the output layer. In the NAR neural network structure, a slope time series with a length n is the input to predict the future road slope $y(t)$, as shown in Figure 2.

3.2. Data Acquisition and Training. After the neural network prediction model is designed, it needs to be trained using

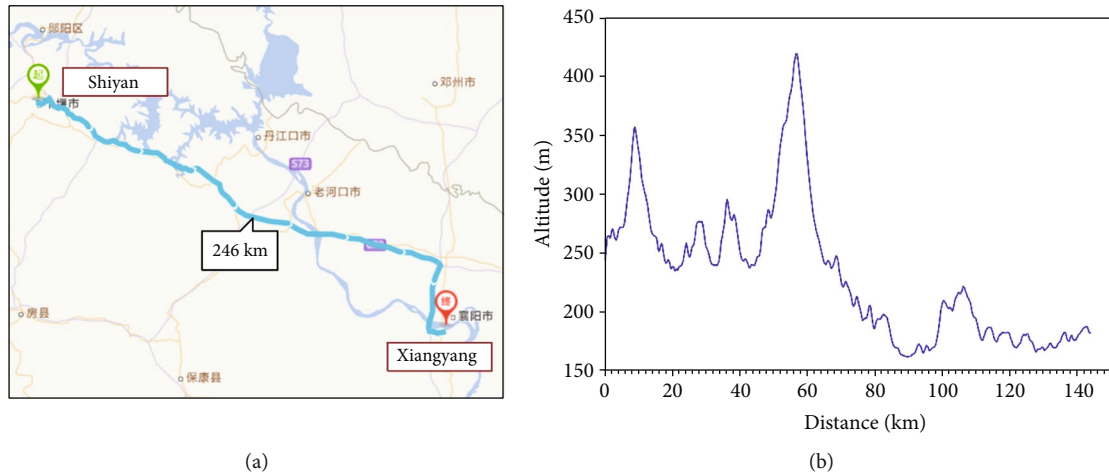


FIGURE 3: The road data used for training and testing: (a) the mark of the expressway on the map and (b) the altitude in the path from Shiyan to Xiangyang.

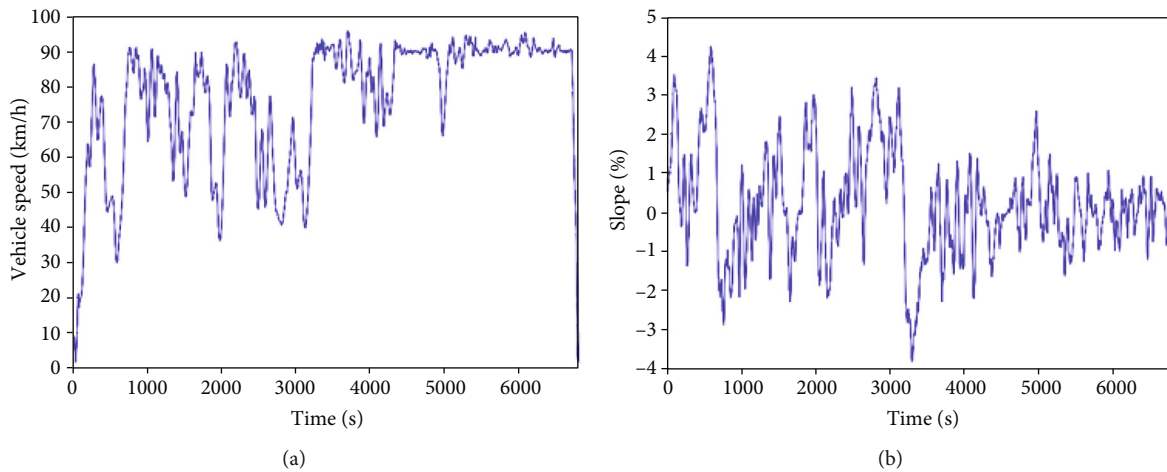


FIGURE 4: The data of the expressway from Shiyan to Xiangyang: (a) the vehicle speed and (b) road gradient.

road slope data. The data used for training and testing are shown in Figure 3; these data were collected on a section of expressway between two cities in China, as shown in Figure 3(a). The distance between the two cities is 246 km. For round trips, the total length of data is 492 km. The road gradient from Shiyan to Xiangyang is shown in Figure 3(b). The average road altitude is higher in the first half of the journey than in the second half of the journey.

As mentioned above, prediction algorithms based on NAR neural networks can only process time-series data. Therefore, based on the vehicle speed for data collection, the altitude in Figure 3(b) is changed to the gradient that varies with time in Figure 4(b), as shown in Figure 4(a). The data acquisition frequency was 1 Hz, and the number of original data samples was 6794. The slope signal changes more sharply than the altitude signal because the slope signal represents the rate of altitude. The first 4500 sampling data points were selected as the training set, and the remaining data were used to test the accuracy of the prediction model.

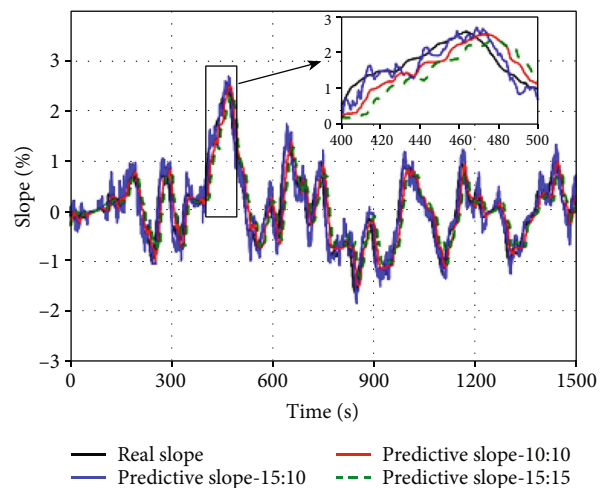


FIGURE 5: Test result of road slope prediction based on the NAR neural network.

TABLE 1: RMSE of the NAR neural network predictive model for different data lengths.

Input: output(s)	15 : 10	10 : 10	15 : 15
RMSE	0.2478	0.3366	0.4511

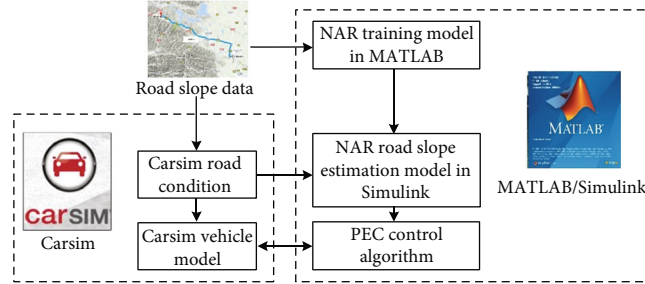


FIGURE 6: The software structure of the real-time simulation.

To find the optimal solution and improve the prediction accuracy, the training data were standardized and normalized. The Z score standardization method was chosen for this study. The maximum number of training steps was set to 200. Furthermore, the gradient threshold was set to 1 to prevent gradient explosions. The learning rate was adjusted by the discrete descent method. The initial learning rate was set to 0.005, which was later increased to 0.2 after the completion of 100 steps. The number of hidden layer nodes was set to 30. After the data processing and the network structure and hyperparameter configuration, the neural network model was trained.

3.3. NAR Neural Network Test. After being trained, the NAR neural network model was tested using the remaining data. To determine the number of input data and the length of predictive time, the results on different settings are compared in Figure 5. Because the prediction horizon of the PEC system was generally set to 10 s or longer, the length of the predictive time of the road slope was set to 10 s or 15 s. For comparison, three test results are given: 15 s input data for 10 s predictive time (represented by predictive slope 15:10), 10 s input data for 10 s predictive time (represented by predictive slope 10:10) and 15 s input data for 15 s predictive time (represented by predictive slope 15:15). The root mean square error (RMSE) of the NAR neural network predictive model for different lengths of input data and output data is shown in Table 1. The smallest RMSE was 0.2478 when the length set was 15:10. In another aspect, vibrations occur when the input data are long. Furthermore, the delay of the results was largest when the length set was 15:15, as shown in Figure 5.

To predict the road slope as quickly as possible, the length set of 15:10 was selected for the control system below. In addition, the input data were not increased further to avoid excessively large vibrations. For offline simulation, the calculation time consumed for NAR conducting one-step prediction was 0.01 s, where the hardware configuration was a 2.5 GHz Intel(R) Core(TM) i7-6500U CPU. The real-time running is validated on the dSPACE platform in the next section.

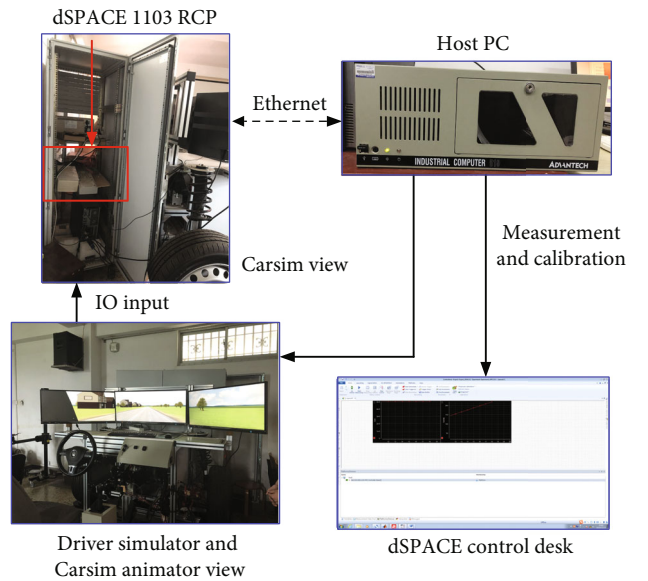


FIGURE 7: The hardware structure of real-time simulation based on dSPACE.

4. Real-Time Simulation on the dSPACE Platform

The software for real-time simulation includes Carsim and MATLAB/Simulink, as shown in Figure 6. The road slope measured in the third section is set in the Carsim road condition and then output to the Simulink model. The neural network algorithm is established in MATLAB first. After training, the neural network algorithm is encapsulated into a Simulink block. Next, the algorithm is simulated for the measured data input, and the road slope prediction result is provided as input for the MPC algorithm established in MATLAB/Simulink. The PEC algorithm is integrated into GRAMPC and runs in MATLAB/Simulink. The optimized output torque was calculated and sent back to the vehicle model in Carsim. Furthermore, the vehicle states and

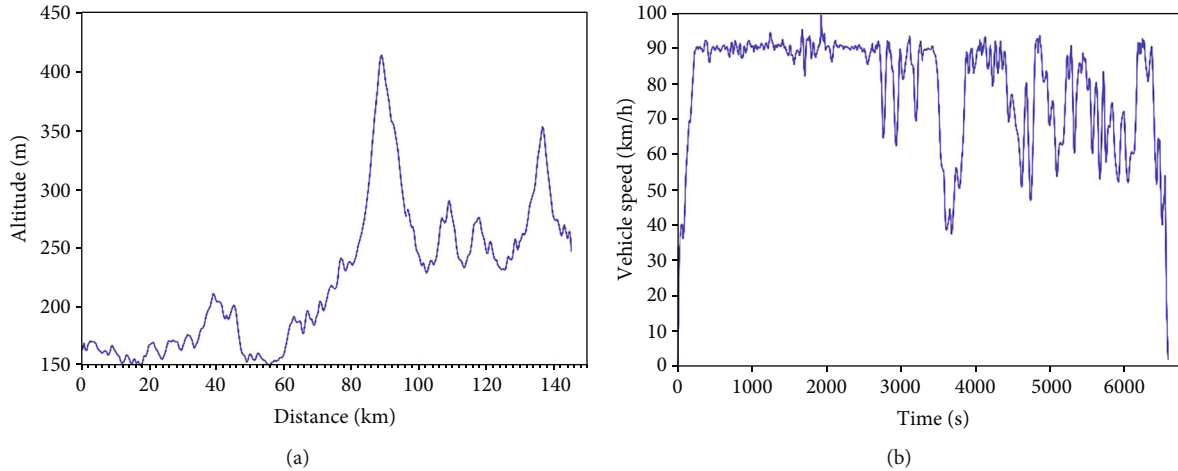


FIGURE 8: The road data for real-time simulation: (a) the road altitude in the path from Xiangyang to Shiyang and (b) the vehicle speed for data collection.

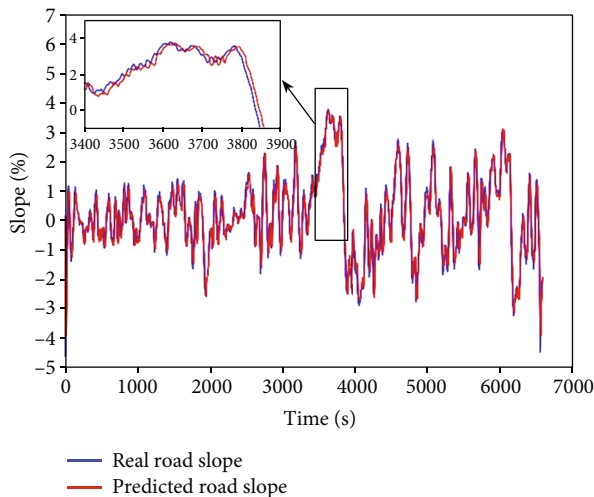


FIGURE 9: Road slope predictive results on the dSPACE real-time platform.

road data are output from Carsim and updated in each MPC iteration.

The real-time simulation platform was established based on the dSPACE 1103 rapid prototyping controller (RCP). The hardware framework is shown in Figure 7. An industrial computer was used as the host computer. The Carsim model, NAR road slope prediction block, and PEC algorithm in Simulink were compiled and loaded into the dSPACE 1103 platform for real-time running. The Carsim real-time running scene was displayed on the driving simulator. The control algorithm and results were measured and calibrated using the Controldesk interface.

Unlike the NAR model training, the road data in the opposite direction (from Xiangyan to Shiyang) were used for the real-time simulation. As a result, the road slope and vehicle speed were different from the data used in the third section. The road altitude and the vehicle speed are shown in Figure 8. The change in road altitude is opposite of that

in Figure 3(b). In addition, the vehicle speed in Figure 8(b) is different from that in Figure 3(a). The vehicle speed for data collection is considered the reference speed to be followed.

The prediction results for road gradients based on the same NAR algorithm trained in the third section are given in Figure 9. Although the vehicle speed is different from that used in the previous training and the route is also different, the prediction model can still effectively predict the slope information. The RMSE of the predictive results is 0.3063. Therefore, the NAR model is generalizable for various types of roads when driving at different speeds.

The simulation results of the variable weight PEC are shown in Figure 10. Figure 10(a) shows that λ_p changes according to the road type. During 3835 s-4400 s and 6140 s-6300 s, the roads are identified as steep downhill roads. The PEC changes λ_p to 0.5, which markedly increases the energy-saving rate. In addition, the vehicle speed can follow the reference speed with a deviation, as shown in Figure 10(b). Due to the inclusion of the minimum power expenditure in the objective costs, the speed of the variable coefficient PEC is smaller than the reference speed.

Compared with the cruise control without PEC, the reduction in energy and the reduction in distance for the same simulation time of PEC on different λ_p are given in Table 2, which shows that the magnitude of λ_p directly correlates with energy savings. However, the reduction in mileage increases with the growth of λ_p . As a result, the two control objectives are in conflict and must be balanced. For PEC with variable weight, the decrease in energy can reach 3.58%, and the decrease in distance is 1.60%, which is almost the same as that when $\lambda_p = 0.12$. For the entire range of 246 km, the performance of the variable coefficient PEC is similar to the effects of the fixed weight coefficients. However, the aim of the proposed weight factor adjustment method is to enhance the performance on each type of road, which will be discussed in the following.

To analyze the control performance on each part of the road, the entire path is divided into seven sections according

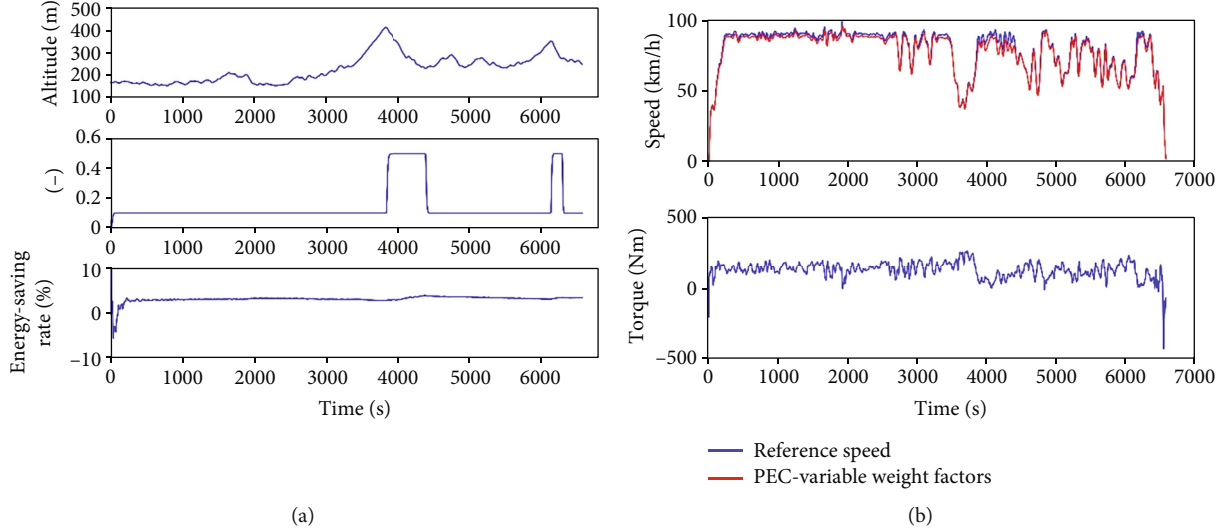


FIGURE 10: Real-time simulation results: (a) elevation, λ_p , and percentage of energy savings and (b) vehicle speed and total torque output.

TABLE 2: Reduction in energy and mileage of PEC for different λ_p .

λ_p	0	0.05	0.1	0.12	0.2	0.3	0.4	0.5	Variable
Δ energy (%)	-1.37	0.44	2.62	3.514	6.92	10.70	14.00	16.92	3.58
Δ time (%)	-0.59	0.06	1.06	1.48	3.13	5.05	6.78	8.36	1.60

to the slope, as shown in Figure 11. Road partition 1 (0-3325 s) is classified as a small uneven road. Road partition 2 (3325 s-3835 s) is a sharply ascending road. Road partition 3 (3835 s-4400 s) is judged to be a sharply descending road according to Equation (5). Road partition 4 (4400 s-5800 s) is the second-smallest uneven road. Road partition 5 (5800 s-6140 s) is the second sharply ascending road. Road partition 6 (6140 s-6300 s) is judged to be the second sharply descending road according to Equation (5). Road partition 7 (6300 s-6585 s) is the third small uneven road. The entire path consists of three types of roads: small uneven roads (segments 1, 4, and 7), sharply descending roads (segments 2 and 5), and sharply ascending roads (segments 3 and 6).

The results of the PEC with a variable weight factor and that of the PEC when $\lambda_p = 0.12$ for each road segment are introduced in Figure 12. Because of the larger λ_p on the sharply descending road, the variable weight method can save more energy on the 3rd road section and the 6th road segment. The energy saving rate is 10% higher on road partition 3 and 14.87% higher on road partition 6. Although the rate at which the distance reduces also increases, the increase is smaller compared with the energy decrease. The mileage is 4.29% smaller on the 3rd road section and 2.7% smaller on the 6th road section. These data indicate that the variable weight PEC can significantly improve the vehicle economic performance while only slightly increasing the traveling time on a sharply descending road.

Because of the smaller λ_p on the other two types of roads, the vehicle economy index of the variable weight method is lower than that of the constant method. However,

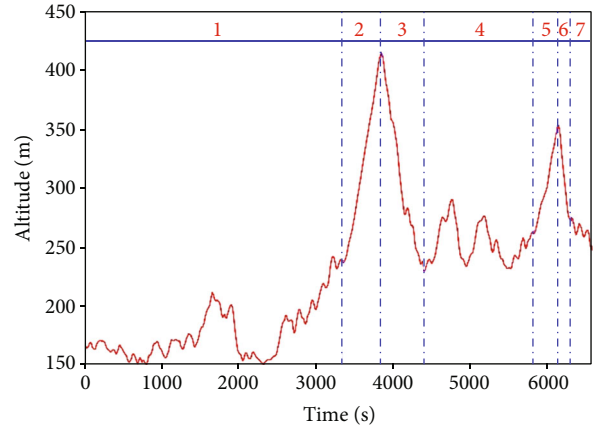


FIGURE 11: Division of the path according to the slope.

the rate at which the distance decreases is also lower. On the remainder of the journey, the overall increase in distance is 1.46% compared with the constant weight method, which helps to improve the time efficiency of driving.

In summary, the variable weight PEC control method increases λ_p to reduce energy consumption on steep downhill roads. The maximum economic improvement can reach 30.87% on road partition 6. On other types of roads, the variable weight PEC control method decreases λ_p to balance the driving time and energy consumption. The overall decreases in energy and mileage are 6.35% and 3.0%, respectively. Thus, the PEC system can better utilize road conditions and exploit the vehicle energy-saving potential.

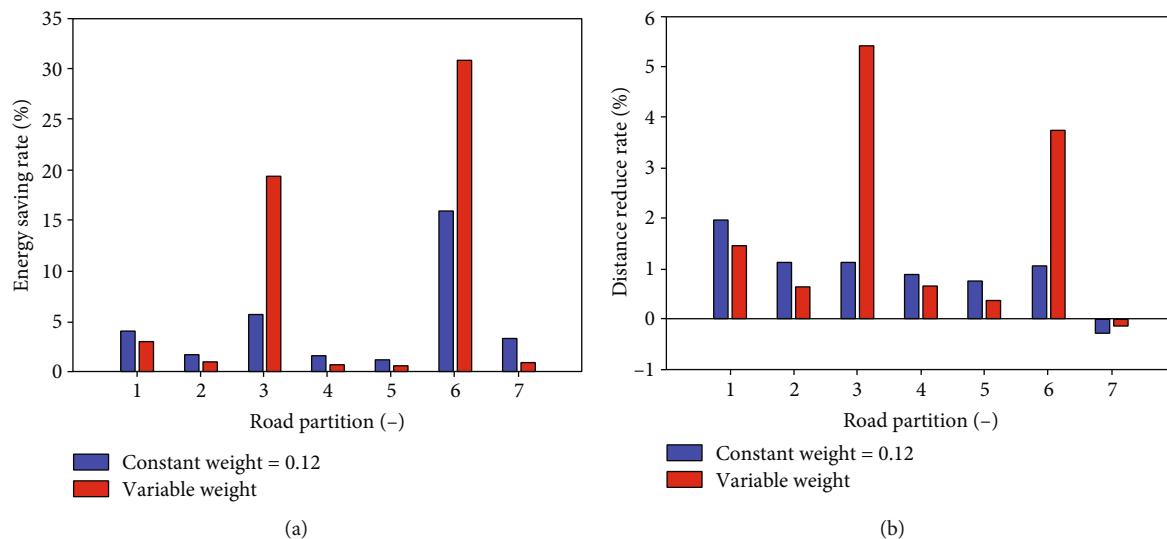


FIGURE 12: Results of variable weight PEC on different types of road segments: (a) reduction in energy and (b) reduction in mileage.

TABLE 3: Comparison of the variable weight PEC and other methods.

Methods	Variable weight PEC	Constant weight PEC		EACC
Maximum Δ energy (%)	30.87%	7.21%	—	—
Δ energy (%)	3.58%	3.53%	8.4%	-0.26%
Δ time (%)	1.6%	0.03%	7.58%	—
Test route	Highway (246 km)	Highway (120 km)	Highway(50 km)	Highway (200 s)
Obtain of road slope	Road slope sensor	MAP+GPS	MAP+GNSS	—
Test method	HIL	Road experiment	HIL	Simulation
Literature	This paper	[16]	[10]	[11]

The comparison of the proposed method with several other existing methods is presented in Table 3. The energy consumption and travel time of a vehicle are affected by many factors, such as the vehicle speed and the length of the route. Therefore, studies that used the driving conditions closest to the ones in this paper were selected. The four methods compared are all tested on the highway. Comparing the PEC and EACC shows that EACC saves little energy on the highway because of the high efficiency of the driving system, which makes it difficult for EACC to save energy by enhancing the driving efficiency. For variable weight PEC and constant-weight PEC, the energy-saving rates of the two methods are similar. However, the maximum energy saving rate of the variable weight PEC is much larger than that of the constant-weight PEC, which facilitates the adaptability of PEC on the different ramps of road. For instance, when the vehicle drives on a short route downhill, the energy-saving effect will be maximized. From the perspective of the entire system solution, the road slope is obtained from the road slope sensor, which is less costly and can be applied over a wider area than the solution based on MAP and GPS or the global navigation satellite system (GNSS). In addition, the proposed PEC strategy in this paper was tested on the HIL platform, which is an important validation step before application to a real vehicle.

5. Discussion

This paper proposes a road slope prediction method using the on-board road slope sensor, which is less costly and can be applied over a wider area than the solution based on MAP and GPS/GNSS. Based on the recorded slope of the road passed before a period of time, the NAR neural network is adopted to establish the road slope predictive model. The results of offline simulation and real-time testing based on the measured road data validated the performance of the proposed road slope predictive method. However, the algorithm was not tested on a real vehicle in a road environment. The noise and delay in the real sensor signal should be further considered in the predictive model.

This paper devised a variable weight PEC algorithm to balance the energy consumption and travel time. The results of the proposed method were compared with other existing methods, which showed that the maximum energy saving rate of the variable weight PEC is much larger than that of the constant-weight PEC. If the vehicle drives on a short route with much downhill movement, the energy-saving effect will be maximized. In future research, the proposed variable weight PEC can be equipped on a real vehicle for further validation.

Other factors can be researched to regulate the weight coefficients of PEC.

6. Conclusions

This research provides some practical solutions for the application of the PEC method in production vehicles. First, the road slope prediction method, using a neural network model based on road slope sensors, was generalizable to various types of roads when driving at different speeds. This approach can be an alternative low-cost solution for obtaining road gradients ahead of production vehicles. Second, PEC can significantly save energy on a grade highway, while EACC has difficulty further optimizing the driving efficiency. On a steep downhill road, the energy saving rate is particularly significant, where the weight factors of the energy savings for PEC should be increased. Compared with the PEC with fixed cost factors, the two control objectives of energy savings and traveling time can be better balanced on various types of roads.

Nomenclature

x_1 :	Vehicle speed
x_2 :	Traveling displacement
δ :	Rotational mass conversion factor
m :	Vehicle mass
T_w :	Required vehicle torque
T_i :	Torque of each in-wheel motor
g :	Gravitational acceleration
f :	Rolling resistance coefficient
α :	Road slope angle
C_D :	Air resistance coefficient
A :	Vehicle windward area
ρ :	Air density
$P_l(T_i, n)$:	Power loss of electric motor
n :	Rotation speed of in-wheel motor,
T :	Prediction horizon
$v_{\text{ref}}(t)$:	Reference speed
T_{min} :	Minimum output torque of each electric motor
T_{max} :	Maximum output torque of each electric motor
λ_p :	Weight coefficient of the minimum energy consumption
λ_v :	Weight coefficient of the minimum speed following deviation
$y(t)$:	Output of the neural network at time t
$\theta(i)$:	Road gradient at the present control step i
PEC:	Predictive energy-saving control
4WD:	Four-wheel-drive
ADAS:	Advanced driving assistance systems
ACC:	Adaptive cruise control
PCC:	Predictive cruise control
EVs:	Electric vehicles
GPS:	Global positioning system
MPC:	Model predictive control
NAR:	Nonlinear autoregressive
GRAMPC:	Gradient-based MPC
RCP:	Rapid prototyping controller
GNSS:	Global Navigation Satellite System.

Data Availability

The data used to support the findings of this study are available from the corresponding author upon request.

Conflicts of Interest

The authors declare that they have no conflicts of interest.

Acknowledgments

This work was supported by the National Natural Science Foundation of China (grant number 51975434) and Foshan Xianhu Laboratory of the Advanced Energy Science and Technology Guangdong Laboratory (grant number XHD2020-003).

References

- [1] A. Boretti, "Plug-in hybrid electric vehicles are better than battery electric vehicles to reduce CO2 emissions until 2030," *International Journal of Energy Research*, vol. 46, no. 14, pp. 20136–20145, 2022.
- [2] M. R. Çorapsız and H. Kahveci, "Double adaptive power allocation strategy in electric vehicles with battery/supercapacitor hybrid energy storage system," *International Journal of Energy Research*, vol. 46, no. 13, pp. 18819–18838, 2022.
- [3] W. Liu, X. Lu, X. Xia, Y. Lu, L. Gao, and Y. Zhuoping, "Automated vehicle sideslip angle estimation considering signal measurement characteristic," *IEEE Sensors Journal*, vol. 21, no. 19, pp. 21675–21687, 2021.
- [4] W. Liu, X. Lu, X. Xia, Y. Lu, L. Gao, and S. Song, "Vision-aided intelligent vehicle sideslip angle estimation based on a dynamic model," *IET Intelligent Transport Systems*, vol. 14, no. 10, pp. 1183–1189, 2020.
- [5] X. Xia, X. Lu, Y. Huang et al., "Estimation on IMU yaw misalignment by fusing information of automotive onboard sensors," *Mechanical Systems and Signal Processing*, vol. 162, p. 107993, 2022.
- [6] S. Dong, B. Gao, Q. Liu, J. Liu, and H. Chen, "A computationally efficient predictive cruise control for automated electric vehicles," *IFAC-PapersOnLine*, vol. 53, no. 2, pp. 14173–14178, 2020.
- [7] D. He and B. Peng, "Gaussian learning-based fuzzy predictive cruise control for improving safety and economy of connected vehicles," *IET Intelligent Transport Systems*, vol. 14, no. 5, pp. 346–355, 2020.
- [8] S. Xu, S. E. Li, H. Peng, B. Cheng, X. Zhang, and Z. Pan, "Fuel-saving cruising strategies for parallel HEVs," *IEEE Transactions on Vehicular Technology*, vol. 65, no. 6, pp. 4676–4686, 2016.
- [9] Z. H. Xu, J. Li, F. Xiao et al., "Energy-saving model predictive cruise control combined with vehicle driving cycles," *International Journal of Automotive Technology*, vol. 23, no. 2, pp. 439–450, 2022.
- [10] P. Gáspár and B. Németh, *Predictive Cruise Control for Road Vehicles Using Road and Traffic Information*, Springer International Publishing, 2019.
- [11] F. Lattemann, K. Neiss, S. Terwen, and T. Connolly, "The predictive cruise control—a system to reduce fuel consumption of heavy duty trucks," *SAE Transactions*, pp. 139–146, 2004.

- [12] H. Erik, J. Åslund, and L. Nielsen, "Design of an efficient algorithm for fuel-optimal look-ahead control," *Control Engineering Practice*, vol. 18, no. 11, pp. 1318–1327, 2010.
- [13] J. D. Gonder, *Route-based control of hybrid electric vehicles. Vol. 1. No. NREL/CP-540-42557*, National Renewable Energy Lab. (NREL), Golden, CO (United States), 2008.
- [14] L. Johannesson and B. Egardt, "A novel algorithm for predictive control of parallel hybrid powertrains based on dynamic programming," *IFAC Proceedings Volumes*, vol. 40, no. 10, pp. 343–350, 2007.
- [15] D. Wu, Y. Li, D. Changqing et al., "Fast velocity trajectory planning and control algorithm of intelligent 4WD electric vehicle for energy saving using time-based MPC," *IET Intelligent Transport Systems*, vol. 13, no. 1, pp. 153–159, 2019.
- [16] E. Hellström, M. Ivarsson, J. Åslund, and L. Nielsen, "Look-ahead control for heavy trucks to minimize trip time and fuel consumption," *Control Engineering Practice*, vol. 17, no. 2, pp. 245–254, 2009.
- [17] P. Sahlholm and K. H. Johansson, "Road grade estimation for look-ahead vehicle control using multiple measurement runs," *Control Engineering Practice*, vol. 18, no. 11, pp. 1328–1341, 2010.
- [18] H. Chu, L. Guo, B. Gao, H. Chen, N. Bian, and J. Zhou, "Predictive cruise control using high-definition map and real vehicle implementation," *IEEE Transactions on Vehicular Technology*, vol. 67, no. 12, pp. 11377–11389, 2018.
- [19] H. S. Bae, J. Ryu, and J. C. Gerdes, "Road grade and vehicle parameter estimation for longitudinal control using GPS," in *Proceedings of the IEEE Conference on Intelligent Transportation Systems*, Oakland CA, USA., 2001.
- [20] R. Labayrade, D. Aubert, and J.-P. Tarel, "Real time obstacle detection in stereovision on non flat road geometry through "v-disparity" representation," in *Intelligent Vehicle Symposium*, vol. 2, Versailles, France, 2002.
- [21] J. Hahn, R. Rajamani, S. You, and K. I. Lee, "Real-time identification of road-bank angle using differential GPS," *IEEE Transactions on Control Systems Technology*, vol. 12, no. 4, pp. 589–599, 2004.
- [22] W. Liu, X. Lu, X. Xia, and Y. Zhuoping, "Intelligent vehicle sideslip angle estimation considering measurement signals delay," in *2018 IEEE Intelligent Vehicles Symposium (IV)*, Changshu, China, 2018.
- [23] L. Gao, X. Lu, X. Lin et al., "Multi-sensor fusion road friction coefficient estimation during steering with Lyapunov method," *Sensors*, vol. 19, no. 18, p. 3816, 2019.
- [24] L. Gao, X. Lu, X. Xia, Y. Lu, Z. Yu, and A. Khajepour, "Improved vehicle localization using on-board sensors and vehicle lateral velocity," *IEEE Sensors Journal*, vol. 22, no. 7, pp. 6818–6831, 2022.
- [25] I. V. Kolmanovsky and D. P. Filev, "Terrain and traffic optimized vehicle speed control," *IFAC Proceedings Volumes*, vol. 43, no. 7, pp. 378–383, 2010.
- [26] H. Chu, L. Guo, H. Chen, and B. Gao, "Optimal car-following control for intelligent vehicles using online road-slope approximation method," *SCIENCE CHINA Information Sciences*, vol. 64, no. 1, pp. 1–16, 2021.
- [27] X. Lu, X. Xia, Y. Lu et al., "IMU-based automated vehicle slip angle and attitude estimation aided by vehicle dynamics," *Sensors*, vol. 19, no. 8, p. 1930, 2019.
- [28] X. Xia, X. Lu, W. Liu, and Y. Zhuoping, "Automated vehicle attitude and lateral velocity estimation using a 6-D IMU aided by vehicle dynamics," in *2018 IEEE Intelligent Vehicles Symposium (IV)*, Changshu, China, 2018.
- [29] C. Lv, X. Yang, J. Zhang et al., "Levenberg–Marquardt back-propagation training of multilayer neural networks for state estimation of a safety-critical cyber-physical system," *IEEE Transactions on Industrial Informatics*, vol. 14, no. 8, pp. 3436–3446, 2018.
- [30] X. Xia, E. Hashemi, X. Lu, and A. Khajepour, "Autonomous vehicle kinematics and dynamics synthesis for sideslip angle estimation based on consensus Kalman filter," *IEEE Transactions on Control Systems Technology*, vol. 31, no. 1, pp. 179–192, 2023.
- [31] X. Lu, X. Xia, Y. Lu et al., "IMU-based automated vehicle body sideslip angle and attitude estimation aided by GNSS using parallel adaptive Kalman filters," *IEEE Transactions on Vehicular Technology*, vol. 69, no. 10, pp. 10668–10680, 2020.
- [32] A. Haddad and O. Mohamed, "Qualitative and quantitative comparison of three modeling approaches for a supercritical once-through generation unit," *International Journal of Energy Research*, vol. 46, no. 14, pp. 20780–20800, 2022.
- [33] Y. Chen, C. Li, S. Chen, H. Ren, and Z. Gao, "A combined robust approach based on auto-regressive long short-term memory network and moving horizon estimation for state-of-charge estimation of lithium-ion batteries," *International Journal of Energy Research*, vol. 45, no. 9, pp. 12838–12853, 2021.
- [34] D. Wu, Q. Yuan, D. Changqing, F. Yan, and L. Yang, "Predictive cruise control for 4WD electric vehicle based on dynamic weight factors," *Energy Reports*, vol. 8, pp. 237–246, 2022.
- [35] A. Domahidi, A. U. Zraggen, M. N. Zeilinger, M. Morari, and C. N. Jones, "Efficient interior point methods for multistage problems arising in receding horizon control," in *2012 IEEE 51st IEEE conference on decision and control (CDC)*, Maui, HI, USA, 2012.
- [36] M. Ramaraj and R. Sivakumar, "Remote sensing and nonlinear auto-regressive neural network (NARNET) based surface water chemical quality study: a spatio-temporal hybrid novel technique (STHNT)," *Bulletin of Environmental Contamination and Toxicology*, vol. 110, no. 1, p. 28, 2023.